Evaluation of the ^{235}U prompt fission neutron spectrum including a detailed analysis of experimental data and improved model information

Denise Neudecker[a], Patrick Talou, Albert C. Kahler, Morgan C. White, and Toshihiko Kawano

Los Alamos National Laboratory, Los Alamos, NM 87545, USA

Abstract. We present an evaluation of the ^{235}U prompt fission neutron spectrum (PFNS) induced by thermal to 20-MeV neutrons. Experimental data and associated covariances were analyzed in detail. The incident energy dependence of the PFNS was modeled with an extended Los Alamos model combined with the Hauser-Feshbach and the exciton models. These models describe prompt fission, pre-fission compound nucleus and pre-equilibrium neutron emissions. The evaluated PFNS agree well with the experimental data included in this evaluation, preliminary data of the LANL and LLNL Chi-Nu measurement and recent evaluations by Capote et al. and Rising et al. However, they are softer than the ENDF/B-VII.1 (VII.1) and JENDL-4.0 PFNS for incident neutron energies up to 2 MeV. Simulated effective multiplication factors $k_{\rm eff}$ of the Godiva and Flattop-25 critical assemblies are further from the measured $k_{\rm eff}$ if the current data are used within VII.1 compared to using only VII.1 data. However, if this work is used with ENDF/B-VIII.0β2 data, simulated values of $k_{\rm eff}$ agree well with the measured ones.

1. Introduction

The prompt fission neutron spectrum (PFNS) of ^{235}U is a quantity of interest for reactor physics and global security. Thus, it has been a subject of in-depth study within an IAEA coordinated research project on "PFNS of actinides" [1]. The ^{235}U PFNS at an incident neutron energy $E_{\rm inc}$ = thermal was also selected as a reference PFNS within the standards project and a preliminary evaluation by Capote et al. [2]—mainly based on experimental data—is available. This evaluation and a recent one by Rising et al. [3] for $E_{\rm inc} \leq 5$ MeV support both a softer PFNS than the ENDF/B-VII.1 [4] (VII.1) and JENDL-4.0 [5] PFNS. The current β2 version of ENDF/B-VIII.0 [6] (VIII.0β2) contains Capote et al. data for $E_{\rm inc}$ = thermal, Rising et al. data for 0.5–5 MeV and VII.1 data above.

Here, we present an evaluation of the ^{235}U PFNS induced by thermal to 20-MeV neutrons. This evaluation is based on modeling all physics processes relevant for this incident energy range, and a detailed analysis of experimental data and their uncertainties, which are briefly summarized in Sect. 2. Evaluated results are shown in Sect. 3 compared to data of VII.1, VIII.0β2, JENDL-4.0 and Rising et al. [3] at $E_{\rm inc}$ = thermal. The evaluated data were used to simulate the effective multiplication factors of the Godiva and Flattop-25 critical assemblies presented in Table 1.

2. Input for evaluation

The vector of evaluated data $\boldsymbol{\psi}$ and the associated covariance matrix $\mathbf{Cov}^{\psi}$ are obtained by a generalized least squares algorithm,

$$\begin{aligned} \boldsymbol{\psi} &= \boldsymbol{\chi} + \mathbf{Cov}^{\psi}\mathbf{S}^t(\mathbf{Cov}^N)^{-1}(\boldsymbol{N}-\boldsymbol{S}\boldsymbol{\chi}), \\ \mathbf{Cov}^{\psi} &= \mathbf{Cov}^{\chi} - \mathbf{Cov}^{\chi}\boldsymbol{S}^t Q^{-1}\boldsymbol{S}\mathbf{Cov}^{\chi}, \\ Q &= \boldsymbol{S}\mathbf{Cov}^{\chi}\boldsymbol{S}^t + \mathbf{Cov}^N, \end{aligned} \quad (1)$$

which combines experimental data $\boldsymbol{N}$, model values $\boldsymbol{\chi}$ and their covariances $\mathbf{Cov}^N$ and $\mathbf{Cov}^{\chi}$. The design matrix $\boldsymbol{S}$ and its transpose $\boldsymbol{S}^t$ are calculated by linear interpolation [7] and account for the outgoing neutron energy E and $E_{\rm inc}$ of experimental data and model values.

Experimental data and uncertainties: The ten experimental data sets [8–16] shown in Fig. 1 are considered for the evaluation. They cover outgoing neutron energies E = 0.1–14 MeV and $E_{\rm inc}$ from thermal to 2.9 MeV.

The experimental covariance matrix $\mathbf{Cov}^N$ was estimated by partitioning the uncertainties of each experiment (with standard deviations Δ^k) according to their k sources, estimating associated correlations $\mathrm{Cor}^k_{i,j}$ for uncertainties between data points i and j and combining them to $\mathrm{Cov}^N_{ij} = \sum_k \Delta^k_i \mathrm{Cor}^k_{i,j} \Delta^k_j$. The covariance matrix between the same and different experiments shown in Fig. 2 was estimated using the newly developed uncertainty quantification program for experimental data "ARIADNE". This program is being developed to facilitate estimating detailed uncertainties and covariances of experimental data. To date, it includes the uncertainty quantification algorithms of Section III.M of [1] for estimating PFNS uncertainties. It will be extended in the future to estimate uncertainties of other observables.

Additional uncertainties were included in $\mathbf{Cov}^N$ based on MCNP studies [17,18] of the experiments highlighted in Fig. 1. These MCNP studies uncovered possible biases

[a] e-mail: dneudecker@lanl.gov

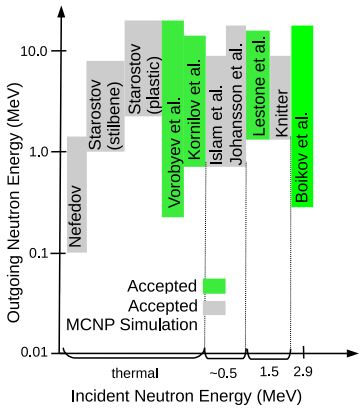

Figure 1. The incident and outgoing neutron energy range of the experimental data used for this evaluation is illustrated.

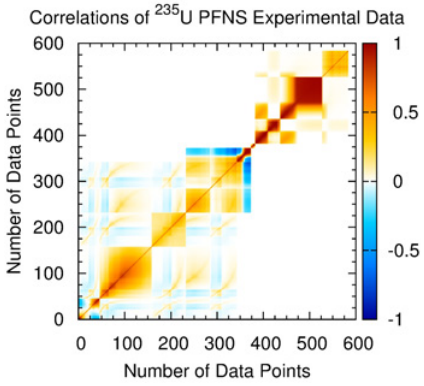

Figure 2. The correlation matrix estimated for the experimental database illustrated in Fig. 1 is shown.

due to the underestimated multiple scattering of neutrons in the surrounding material and the sample as well as an inadequate deconvolution of the PFNS when transforming from time-of-flight to energy.

Model information: The "CoH" code [19] was used to calculate model PFNS $\boldsymbol{\chi}$ for first and multiple-chance fission processes and the associated covariance matrix $\mathbf{Cov}^{\chi}$ by means of the Los Alamos model [20] combined with the Hauser-Feshbach [21] and exciton models [22]. The total spectrum χ in the laboratory frame, considering up to 4$^{\text{th}}$-chance fission processes, is given by

$$\chi(E) = \frac{\sum_{i=1}^{4} P_{fi}\left[\nu_i \chi_i(E) + \sum_{j=1}^{i-1} \phi_j(E)\right]}{\sum_{i=1}^{4} P_{fi}[\nu_i + i - 1]}. \quad (2)$$

The spectra $\phi_j(E)$ are the pre-fission neutron spectra of $j = \{1, 2, 3\}$ neutron(s) emitted before fission in compound and pre-equilibrium processes as described in Ref. [7]. The variables P_{fi} correspond to the $i = \{1^{\text{st}}, 2^{\text{nd}}, 3^{\text{rd}}, 4^{\text{th}}\}$-chance fission probabilities. They are calculated by fitting fission barrier heights and curvatures to P_{fi} obtained from VII.1 ^{235}U total and i^{th}-chance fission cross sections. The spectra χ_i are weighted with P_{fi} and ν_i, the average number of neutrons emitted. The spectra $\chi_i(E)$ are those of neutrons emitted promptly from the i^{th}-chance fission fragments.

The first-chance fission spectrum $\chi_1(E)$ is described by an extended LAM [23] as a sum of effective light and heavy fission fragment neutron emission spectra, χ_{L1} and χ_{H1}, weighted with the average light and heavy neutron multiplicities, ν_{L1} and ν_{H1}, $\chi_1(E) = (\nu_{L1}\chi_{L1}(E) + \nu_{H1}\chi_{H1}(E))/(\nu_{L1} + \nu_{H1})$. Here, ^{96}Sr and ^{140}Xe are used as effective light and heavy fission fragments with ν_{L1}/ν_{H1} =1.2. The effective light or heavy fission fragment neutron spectrum, χ_{x1} with subscript $x = \{L, H\}$, is calculated by

$$\chi_{x1}(E) = \frac{\int_{(\sqrt{E}-\sqrt{E_f})^2}^{(\sqrt{E}+\sqrt{E_f})^2} \sigma_{c,x}(\varepsilon)\sqrt{\varepsilon}\left(1 + b\frac{(E-\varepsilon-E_f)^2}{4\varepsilon E_f}\right) I(\varepsilon)\mathrm{d}\varepsilon}{2\sqrt{E_f}\,T_{m,x}^2(1 + b/3)}, \quad (3)$$

with the temperature distribution $I(\varepsilon)$ of [24]. The variable E_f denotes the kinetic energy per nucleon of the fission fragments and $\sigma_{c,x}$ the inverse compound nucleus formation cross section. The maximum temperature of the fission fragments is given by $T_{m,x} = \sqrt{\langle E^* \rangle / \langle a_x \rangle}$, with the average level density parameter $\langle a_x \rangle = A_x/11$ dependent on the mass number A_x. The average total excitation energy $\langle E^* \rangle = \langle E_r \rangle + E_{\text{inc}} + B_n - \langle TKE \rangle$ is calculated from the average energy release $\langle E_r \rangle$, E_{inc}, the neutron binding energy B_n and the total kinetic energy $\langle TKE \rangle$ averaged over the fission fragment distribution. A value of 170.5 MeV is taken for $\langle TKE \rangle$ at E_{inc} = thermal and a linear decrease is assumed for higher E_{inc}. The slope of this linear function was obtained by fitting to $\langle TKE \rangle$ data of [25]. The energy release is parametrized following Ref. [26]. The parameter b in Eq. (3) defines the strength of the anisotropy of the neutron evaporation in the center-of-mass frame with center-of-mass energy ε and assumes a value of 0.1. For multiple-chance fission spectra $\chi_i(E)$ with $i > 1$, the average excitation energy of the pre-fission nucleus is corrected for the energy removed by the pre-fission neutrons. The covariances $\mathrm{Cov}^{\chi}(E_i.E_j)$ associated with model values $\boldsymbol{\chi}$ are calculated by sampling parameter values $\boldsymbol{p}_l$, calculating $\boldsymbol{\chi}(\boldsymbol{p}_l)$ and computing from those the covariance estimator as described in Ref. [7].

3. Results

Evaluated results: The evaluated PFNS at E_{inc} = thermal in Fig. 3 agrees well with experimental data of [8–11], the Rising et al. and the VIII.0β2 evaluation (Capote et al.) within its 1-σ uncertainty bounds. It is distinctly softer than the VII.1 and JENDL-4.0 evaluations. This trend to a softer PFNS can also be observed for E_{inc} = 1.5 MeV. The data of Lestone et al. [14] and Knitter et al. [15] agree similarly well with all three evaluations. However, the preliminary Chi-Nu data [27]—which are not included in any of these evaluations—support a PFNS softer than VII.1. The higher evaluated PFNS at low E is partially caused by extension made to the LAM as shown in Ref. [23], but also by the experimental database chosen. The latter point is supported by the agreement of this evaluation with VIII.0β2 at E_{inc} = thermal, which is mainly based on experimental data. Both evaluations include data of the Starostov et al. measurement series [8,9] which were not considered for the VII.1 evaluation.

At E_{inc} = 6 and 14 MeV, this evaluation shows similar structures as JENDL-4.0 data, whereas VII.1 data are smooth. The peak from E =6–8 MeV at E_{inc} = 14 MeV is caused by neutrons emitted in a pre-equilibrium process, which are considered in this evaluation and JENDL-4.0 but not in VII.1. The increase of the PFNS around a few

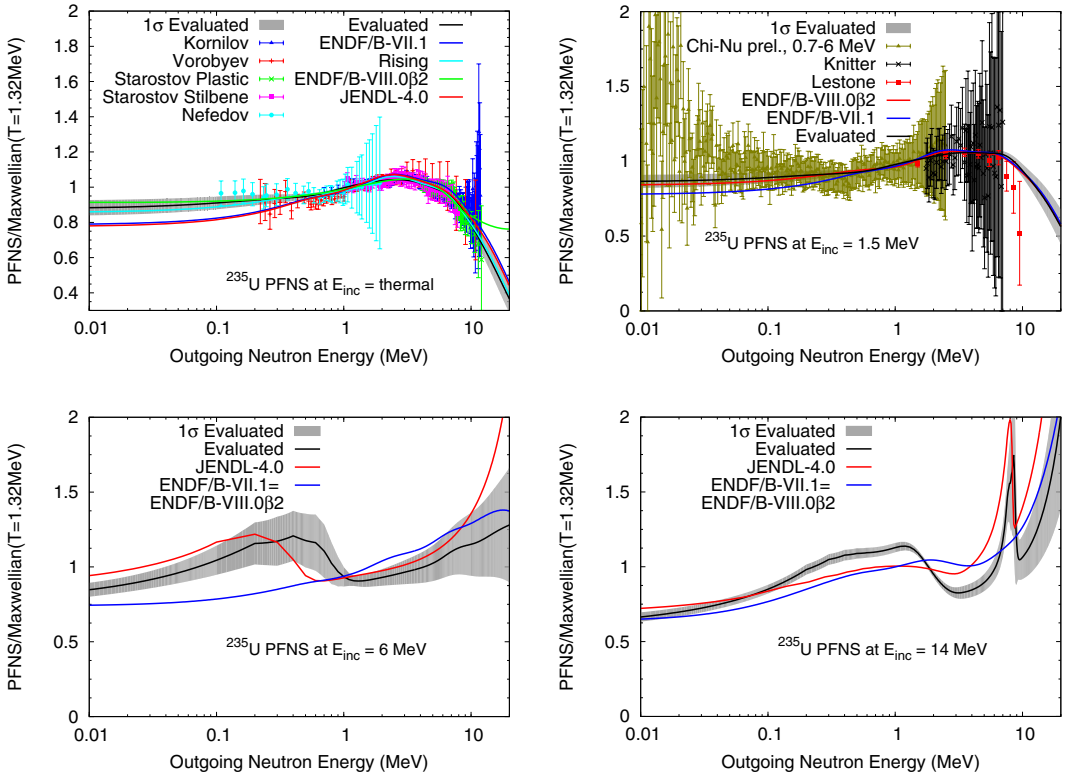

Figure 3. The evaluated ^{235}U PFNS of this work are compared to experimental data of [8–11, 14, 15], preliminary Chi-Nu data [27] and evaluations of [2–6] for $E_{\rm inc}$ = thermal, 1.5, 6 and 14 MeV. Experimental data are scaled with respect to this work.

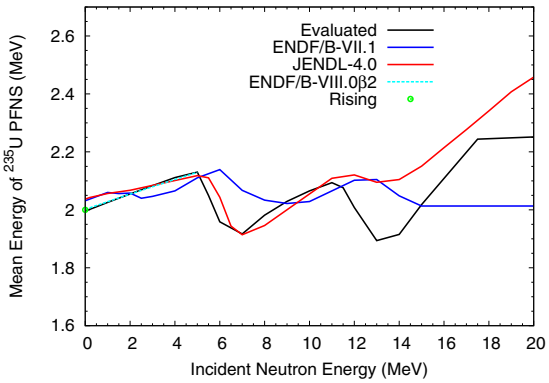

Figure 4. Evaluated mean energies of this work are compared to those of VII.1, VIII.0β2 (only shown, where different from VII.1), JENDL-4.0 and the evaluation of [3] at $E_{\rm inc}$ = thermal.

hundred keV at $E_{\rm inc}$ = 6 MeV arises from the fact that only pre-fission and prompt fission neutrons are counted [7].

The tendency of this evaluation to softer PFNS compared to VII.1 and JENDL-4.0 for $E_{\rm inc} \leq 2$ MeV is also visible in the evaluated mean energies in Fig. 4. The evaluated mean energies are nearly the same as those calculated from the VIII.0β2 evaluation for $E_{\rm inc} \leq 5$ MeV. The mean energies of this work agree qualitatively with the JENDL-4.0 evaluation for $E_{\rm inc}$ = 5–11 MeV. Above $E_{\rm inc}$ = 11 MeV, the evaluated mean energies differ widely. No experimental data are currently available to guide evaluations for $E_{\rm inc} >$ 11 MeV, but the Chi-Nu project might provide insight in the future.

Benchmarking results: If the current evaluated results are used with VII.1 data for all other isotopes and ^{235}U observables, the MCNP6.1.1 [28] calculated effective multiplication factor $k_{\rm eff}$ of Godiva is higher by 29 pcm, and further from unity, than if only VII.1 data are used. This slightly worse $k_{\rm eff}$ was expected as VII.1 data are adjusted to yield a simulated value close to the measured Godiva benchmark. In addition, this evaluation differs visibly from the VII.1 PFNS in Fig. 3 leading to differences in the simulated $k_{\rm eff}$. An effect of a similar size (31 pcm) can be observed for $k_{\rm eff}$ of Flattop-25 in Table 1.

However, if this evaluation is used with VIII.0β2 data, the simulated $k_{\rm eff}$ of Godiva is very close to unity and differs from the value simulated with only VIII.0β2 data within the Monte Carlo (MC) sampling uncertainties. The Flattop $k_{\rm eff}$ simulated with VIII.0β2 data are improved by more than 200 pcm compared to values simulated with VII.1. Again, $k_{\rm eff}$ factors differ within their MC sampling uncertainties if simulated with this evaluation combined with VIII.0β2 compared to using only VIII.0β2. These similar values of $k_{\rm eff}$ concur with the fact that the VIII.0β2 PFNS and the current evaluation agree for $E_{\rm inc} \leq$ 5 MeV within the evaluated uncertainties of this work (see Figs. 3–4).

Table 1. MCNP6.1.1 [28] calculated $k_{\rm eff}$ factors of the Godiva (HMF001) and Flattop-25 (HMF028) critical assemblies are given. Data of VII.1, VII.1 combined with this evaluation (TE), VIII.0β2 and VIII.0β2 combined with this evaluation were used for the calculations. The MC sampling uncertainties are given in pcm in parentheses.

Data	HMF001	HMF028
VII.1	1.00002(8)	1.00299(9)
VII.1+TE	1.00031(8)	1.00268(9)
VIII.0β2	1.00009(8)	1.00081(9)
VIII.0β2+TE	1.00008(8)	1.00067(9)

4. Summary and outlook

An evaluation of the ^{235}U PFNS induced by neutrons of thermal to 20 MeV was presented. The covariances of experimental data [8–16] were estimated in detail using information provided in Refs. [17,18]. The Los Alamos model [20] combined with the Hauser-Feshbach [21] and the exciton models [22] were used to model prompt fission, pre-fission compound nucleus and pre-equilibrium neutron emissions. The evaluated results agree reasonably well with PFNS and mean energies of recent evaluations by Capote et al. [2] at $E_{\rm inc}$ = thermal and Rising et al. [3] for $E_{\rm inc} \leq 5$ MeV, which are included in the VIII.0β2 library. The PFNS of these three evaluations are softer than those of VII.1 and JENDL-4.0 for $E_{\rm inc} \leq 2$ MeV (Figs. 3–4). Preliminary Chi-Nu data [27] support this tendency of a softer PFNS. Calculated effective multiplication factors $k_{\rm eff}$ of Godiva and Flattop-25 using this evaluation combined with VIII.0β2 are close to the measured benchmarks (Table 1). The $k_{\rm eff}$ of Flattop-25 is better than the one simulated using VII.1. Further benchmark studies—such as calculating $k_{\rm eff}$ of thermal solution critical assemblies—need to be undertaken.

We thank M.J. Devlin, D.L. Duke, J. Gomez, R.C. Haight, H.Y. Lee, J.P. Lestone, J.M. O'Donnell, T.N. Taddeucci for discussing experimental data, R. Capote, D.L. Smith for discussing evaluation techniques and M.B. Chadwick for his inquisitive interest in this subject. This work was carried out under the auspices of the NNSA of the U.S. Department of Energy at LANL under Contract No. DE-AC52-06NA25396.

References

[1] R. Capote et al., Nucl. Data Sheets **131**, 1 (2016)
[2] A. Trkov, R. Capote, Physics Procedia **64**, 48 (2015)
[3] M.E. Rising et al., Nucl. Sci. Eng. **175**, 81 (2013)
[4] M.B. Chadwick et al., Nucl. Data Sheets **112**, 2887 (2011)
[5] K. Shibata et al., J. Nucl. Sci. Technol. **48**, 1 (2011)
[6] ENDF/B-VIII.0β2: `https://ndclx4.bnl.gov/gf/project/` endf/scmsvn/?action=browse&path=%2F&view=rev& revision=919 (Revision 919)
[7] D. Neudecker et al., Los Alamos National Laboratory Report LA-UR-16-27361 (2016)
[8] V.N. Nefedov et al., INDC Report 0457 (2014), EXFOR-No. 40871.007 & 40871.012
[9] B.I. Starostov et al., INDC Report 0458 (2014), EXFOR-No. 40872.007
[10] A.S. Vorobyev, O.A. Shcherbakov, INDC Report INDC(CCP)-0455 (2014), EXFOR-No. 41597.002
[11] N. Kornilov et al., Nucl. Sci. Eng. **165**, 117 (2010), EXFOR-No. 31692.006
[12] M.M. Islam, H.-H. Knitter, Nucl. Sci. Eng. **50**, 108 (1973), EXFOR-No. 20385.003
[13] P.I. Johansson, B. Holmqvist, Nucl. Sci. Eng. **62**, 695 (1977), EXFOR-No. 20175.003
[14] J.P. Lestone, E.F. Shores, Los Alamos National Laboratory Report LA-UR-14-24087 (2014)
[15] H.-H. Knitter et al., Z. Phy. **257**, 108 (1972), EXFOR-No. 20394.008
[16] G.S. Boikov et al., Sov. J. Nucl. Phys. **53**, 392 (1991), EXFOR-No. 41110.009
[17] T.N. Taddeucci et al., Nucl. Data Sheets **123**, 135 (2015)
[18] D. Neudecker et al., Nucl. Data Sheets **131**, 289 (2016)
[19] T. Kawano et al., J. Nucl. Sci. Technol. **47**, 462 (2010)
[20] D.G. Madland, J.R. Nix, Nucl. Sci. Eng. **81**, 213 (1982)
[21] W. Hauser, H. Feshbach, Phys. Rev. **87**, 366 (1952)
[22] E. Gadioli, P.E. Hodgson, *Pre-equilibrium nuclear reactions* (Clarendon Press, Oxford, UK, 1992)
[23] D. Neudecker et al., Nucl. Instr. Methods in Phys. Res. Sect. A **791**, 80 (2015)
[24] F.-J. Hambsch, et al., Ann. Nucl. Energy **32**, 1032 (2005)
[25] D.L Duke, Los Alamos National Laboratory Report LA-UR-15-28829 (2015)
[26] D.G. Madland, Nucl. Phys. A **772**, 113 (2006)
[27] R.C. Haight et al., Nucl. Data Sheets **123**, 130 (2015)
[28] T. Goorley, Los Alamos National Laboratory Report LA-UR-14-24680 (2014)